BR19 - Reactions and Phase Transformations During the Low-Temperature Reduction of Bauxite Residue by H2 in the Presence of NaOH, and Recovery Rates Downstream

Ganesh Pilla[1], Tobias Hertel[2], Stergi Kapelari[3], Bart Blanpain[4] and Yiannis Pontikes[5]
1. PhD student
2. Postdoc Researcher
3. PhD student
4. Professor
5. Professor
KU Leuven, Department of Materials Engineering, Leuven, Belgium
Corresponding author: ganesh.pilla@kuleuven.be

Abstract

The scope of this work is to investigate the reactions and phase transformations that occur during the low-temperature reduction of bauxite residue (BR) by hydrogen in the presence of NaOH, and how that affects the recovery downstream of the different elements. Different processing conditions were studied, such as temperature, time, and NaOH dosage under a pure hydrogen atmosphere. XRD results revealed that hematite (Fe_2O_3) and goethite (FeOOH) were completely converted to magnetite (Fe_3O_4) when a blend of BR and 20 wt % NaOH was treated at 500 °C for 30 min. The iron recovery and grade of magnetic rich fraction after water leaching -magnetic separation of reduced BR (at 500 °C, 20 wt % NaOH, 30 min reduction time) is 87.7 % and 44.5 % respectively, whereas the aluminum and sodium recovery under these conditions is 75 % and 87 %. The formation of $NaAlO_2$ occurs at 400 °C, and the amount formed increases till 700 °C. When NaOH addition exceeds 25 wt % and the temperature is higher than 600 °C, the formation of water-soluble sodium iron oxide ($NaFeO_2$) and sodium-calcium silicate ($Ca_2Na_2Si_3O_9$) along with wüstite (FeO) takes place. This led to lower Fe and Al recovery and further dissolution of Fe, Si, and Ca in the leach liquor during water leaching and wet-magnetic separation. For thermal processing at 500°C for 30 min with 20 wt % NaOH, the amount of Fe_3O_4 forming is the highest, and via magnetic separation, a Fe-rich fraction is recovered. In the non-magnetic fraction, perovskite ($CaTiO_3$), calcite ($CaCO_3$), and quartz (SiO_2) are enriched, whereas the leach liquor is Na and Al-rich, as confirmed by ICP-OES measurements. The partitioning of rare earth elements in the different phases, as well as what is overall the preferable recovery process, are also discussed.

Keywords: Bauxite residue, Hydrogen, Circular economy, Alkaline roasting, Phase transformations.

1. Introduction

The Bayer processing of bauxite for alumina extraction generates a substantial amount of strong alkaline solid waste known as bauxite residue (BR) or red mud. On average, 1.35 tonnes of alumina produces 0.8-2.5 tonnes of bauxite residue, with global stockpiling expected to reach 5 billion tonnes by 2020 [1]. Currently, most efforts on BR utilization focus on recovering key metals, like iron, aluminum, titanium, and REEs, and on manufacturing building and construction materials. However, the utilization rate is less than 3 %. It is worth noting that the composition of BR can vary depending on the source of the bauxite and the conditions under which it is processed. BR is typically made up of 5-65 % iron oxides, 5-40 % aluminum oxides, 5-40 % silicon oxides, and 3 percent–20 % titanium oxides in addition to a sizable amount of strategic metals like scandium (Sc) and lanthanides as REEs [2]. BR may therefore be regarded as supplementary raw material for the recovery of Fe, Al, Ti, Ca, and REEs. Bauxite, which makes up 70 % to 80 % of

the deposits of scandium, has not been employed as a raw material to extract scandium. BR is enriched with more than 98 % Sc (50–120 mg/kg) [13, 14] during the alumina production from the Bayer process. This has resulted in the recovery of Fe, Al, Ti, and REEs from BR being explored at the laboratory scale with the objective of achieving near-zero waste valorization and carbon footprint. Metal recycling technologies like physical separation by direct magnetic separation, pyrometallurgical procedures including smelting and reduction roasting-magnetic separation, and hydrometallurgical acid leaching techniques, are the broad categories for the recovery of metals.

One technique for recovering iron fractions while leaving behind the non-magnetic fractions (Al, Si, Ti, Ca, Si) of BR is direct magnetic separation [1]. The bulk of hematite and goethite particles are fine, weakly magnetic, and agglomerate with fine non-magnetic minerals of desilication product (DSP), making them difficult to separate from BR. Additionally, the distribution of minerals phases in BR is complicated and the extraction of iron is intertwined with that of other elements. As a result, using physical separation techniques, it is challenging to extract metals from BR. On the other hand, in the hydrometallurgical route, various acids (HCl, H_2SO_4, HNO_3) are used to dissolve elements (including Fe, Al, Ti, Ca, and REEs) in BR by varying the acid dosage, leaching duration, and temperature. However, multielement dissolution complicates downstream separation processes due to complicated flowsheets, huge volume generation of liquid byproducts, high impurity levels, hazardous/corrosive acids, and/or uneconomic process conditions [3,4].

As a result, BR is an intriguing potential resource, with the techniques investigated generally falling within the categories of reduction smelting and reduction roasting. Slag and a product of pig-iron grade are produced when BR is smelted using a reducing agent (carbon) at higher temperatures such as 1400-1800 °C through the smelting reduction process. High energy consumption and operating temperatures, and high sodium content in the raw materials in the smelting process limit commercial manufacturing on an industrial scale [5]. Researchers have extensively explored the popular technique of reductive roasting of BR and other residues at temperatures between 300 to 1000 °C using coke, CO, or hydrogen to separate iron minerals such as Fe_3O_4, and pure Fe [6-12]. A recovery rate of 88 % Fe and grade of 90 % were observed when BR was reduced with carbon at 1000 °C, with the resulting iron possible to use as an ingredient in iron making directly. It has been suggested from previous research methods [6,7,11] that the sodium-based flux (sodium carbonate, sodium hydroxide, and sodium sulfate) during reductive roasting substantially increases the reduction and recovery of Al, Si, and Na-bearing non-magnetic phases via the formation of water-soluble sodium silicate and sodium aluminate phases from reduced BR after magnetic separation and water leaching [6-13]. The low-temperature reduction roasting of BR at 600 °C with hydrogen and addition of NaOH is investigated to recover the pure iron and aluminum simultaneously but lower recovery rates of Al and Fe were observed. Also, it should be noted that the above-mentioned studies do not provide a sufficient explanation of the non-magnetic, magnetic, and REEs phase assemblage and the ongoing transformations in reduction roasting. Additionally, none of the processes showed proof-of-concept for industrial upscaling, confirming that all the above-mentioned technologies are in their infancy. For the alumina industry to grow sustainably and environmentally friendly, an efficient bauxite residue valorization is a key technology.

In the present study, the reduction roasting of BR by adding NaOH at lower temperatures ranging from 400-700 °C under pure hydrogen is investigated by adjusting time (30-120 min), temperature, and NaOH addition (10-25 wt %). Then, the reduced products were processed to combine water leaching and wet magnetic separation method for the recovery and separation of metals such as Fe, Al, Na, Ca, Ti, and Sc. X-ray powder diffractometer (XRD), Rietveld QXRD analysis, scanning electron, microscope-energy dispersive spectroscopy (SEM-EDS), and electron probe micro-analyzer (EPMA) were utilized to investigate the phase transformation,

magnetic transformation, and microstructure variation of the roasting and separation products. The findings of this work can contribute to a better understanding of the phase structural changes in previously researched processes of BR [11,12], and also can give a significant foundation for the recovery of key metals (Fe, Al, Ti, and Sc) from BR in this carbon lean process.

2. Materials & Methods

2.1 Raw Materials

The BR sample used in this study were obtained from the Mytilineos S.A plant in Agios Nikolaos, Greece. The acquired sample was dried in an oven at 110 °C for 12 h to remove the moisture from the BR. To guarantee uniform particle dispersion and removal of large particles, the dry BR was sieved using a 500 µm screen. The particle size distribution was evaluated using a Beckman Coulter LS12320 laser particle size analyzer. The chemical composition of BR was analyzed through Bruker S8 Tiger X-ray fluorescence (XRF) method. Further, X-ray diffraction (XRD) was used to evaluate the mineral phase composition using a Bruker D2 Phaser with Cu-k_α source, 30 kV voltage, 10 mA current from 10° to 65° diffraction angle. To quantify the phases in raw BR, quantitative XRD was performed using Rietveld refinement, by using the TOPAS software's profile fitting approach. SEM EDS was used to analyse the microstructure and microchemistry of BR (SEM Philips XL30 FEG model).

Sodium hydroxide (NaOH) of analytical grade was employed as an additive in the experiments.

2.2 Experimental Methods

Thermodynamic Calculations

Thermodynamic investigation of the reductive roasting of BR in the presence of hydrogen was performed using FactSage8.1™ thermochemical software with the databases of FT-oxid, FT-PS, FT-Salt, and FT-misc were used, which include all of the oxides present in the system, including magnetite and sodium-aluminates. The impact of NaOH addition was investigated on the phase equilibria of 100 g BR at 500 °C with a 3g hydrogen. Also, the process temperature (300-900 °C) and hydrogen (1-5g) amount in the presence of NaOH salts was studied

Low-temperature Reduction

The experimental procedure as shown in Figure 1 includes raw material mixing, pelletization, reduction roasting, and water leaching combined with wet magnetic separation. A 20 ml solution of sodium hydroxide (NaOH) was made by mixing NaOH pellets with water. The NaOH solution was then mixed in Eirich EL-1 type mixer with BR to create pellets ranging in size from 10 to 15 mm.

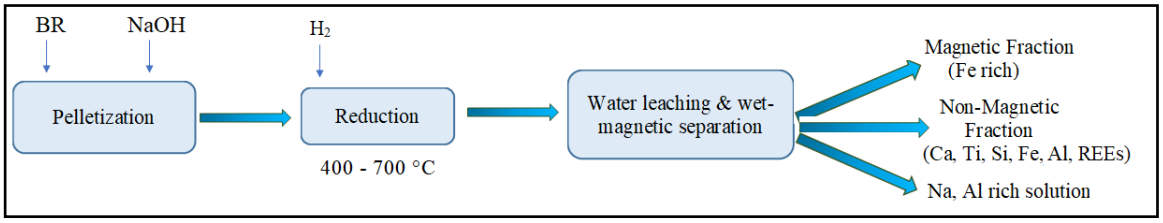

Figure 1. Flow sheet of experimental procedure followed in this work.

A rectangle alumina crucible 100 mm long and 50 mm wide holding roughly 100 g of pellets was inserted in a gas-tight laboratory box furnace. Several factors were investigated to optimize the process, including reduction temperatures (400 - 700 °C), reduction duration (30 - 120 min), and NaOH dose (10 - 25 wt %). At first, the pellets were dried in the furnace for 2 h and the pellets were heated at a rate of 10 °C/min till the desired temperature reaches. The steady flow (20 L/h) of 100 % vol. hydrogen was purged as a reducing agent in each reduction roasting experiment. After reduction, nitrogen gas was injected at a flow rate of 10 l/h to cool down the pellets to room temperature. The temperature within the furnace was measured using a thermocouple. The reduced pellets were wet-milled in an RS200-type vibrating disk mill with water, with a solid: liquid ratio of 1:2.

Water leaching and Wet-magnetic separation

The wet-milled products were then subjected to combined water leaching and wet-magnetic separation process to separate the sodium aluminate solution, magnetic and non-magnetic products, simultaneously. Water leaching was performed at a leaching temperature of 60 °C and duration 60 min. A liquid-to-solid (L/S) (mass) ratio of 10:1 was used. To separate the magnetic-rich product before the filtering process, a solid NdFeB magnet (5 x 5 x 2.5 cm^3) was kept within the water leaching set-up for the effective separation of magnetic and non-magnetic products. After water leaching of products, filtration with 12 µm pore size filter paper was employed to segregate the solid residue from the leach solution. The liquid samples were passed through a 0.45 µm pore size filter before measuring at the ICP-OES. The iron recovery rate was computed using Equation-1. Furthermore, the leach recovery of aluminum and sodium was determined using Equation-2 [15].

$$Fe\ Recovery = \frac{(C*c)}{((C*c)+(t*T))} * 100 \qquad (1)$$

$$Al\ (or)\ Na\ Recovery = \frac{(cL*VL)}{((cL*VL)+(CSR*mSR))} * 100 \qquad (2)$$

where C: weight of the concentrate (grade), c: assay of concentrate (%); T: weight of tailing (grade); t: assay of tailings (%); cL: element concentration in the leachate solution (g/mL); VL: volume of analyzed leachate solution (mL); CSR: elemental concentration in solid residue (mg/g); mSR: weight of solid residue (g). Further the grade of iron was calculated from the XRF iron oxides data based on the below Equation-3.

$$TFe\ (Grade) = \frac{(2*Molecular\ weight\ \ of\ Fe)}{(Molecular\ wt\ of\ hematite)} * Wt\%\ of\ \text{hematite}\ (\ from\ XRF) \qquad (3)$$

Characterization of Products

The phase analysis of the solid products (magnetic and non-magnetic fractions) was carried out using QXRD technique after overnight drying in the oven. The elemental composition of the liquid solutions was analyzed using ICP-OES. The microstructures and elemental distribution of products were examined by using scanning electron microscopy along with equipped energy-dispersive spectroscopy (EDS), and an Electron probe micro-analyzer (EPMA) with 20 kV voltage and 100nA current in the XA-8500 JEOL FTM model of EPMA. The products were embedded in epoxy resin before being ground with silicon carbide papers and polished with oil-based diamond suspension. Further, 15 nm carbon coating was applied to the polished specimens. The chemical composition of the solid products was determined using X-ray fluorescence (XRF).

3. Results and Discussion

3.1 Characterization of Raw BR

The used BR contains significant amounts of iron oxides and alumina (as shown in Table 1) and is a very fine material with a D_{90} of <12 μm and D_{50} of 2.2 μm. XRD revealed that it includes several phases such as hematite, goethite, gibbsite, diaspore, calcite, perovskite, anatase, and cancrinite. The QXRD revealed that the hematite and goethite iron oxide phases account for 34 wt % and 8 wt %, respectively of the raw BR. On the other hand, diaspore and gibbsite are 17 wt % and 2 wt %, respectively. The detailed characterization of raw BR was presented in previous research work [12].

Table 1. Chemical composition of raw BR sample via XRF.

Component	Fe_2O_3	TFe	Al_2O_3	Na_2O	SiO_2	CaO	TiO_2	LOI
Wt %	38.1	27.1	23.6	3.2	7.5	8.2	5.1	11.2

3.2 Thermodynamic Calculations

By using the software Factsage 8.1, the impact of NaOH addition was investigated on the phase equilibria of BR at 500 °C with 3g of hydrogen as input. The development of water-leachable sodium iron oxide ($NaFeO_2$) is facilitated by the addition of higher additions of NaOH (>20 wt %). The phase stability of water leachable phases of $NaFeO_2$, $NaAlO_2$, and Na_2SiO_3 increases with increasing NaOH. It can be concluded that 20 wt % of NaOH is sufficient to react with BR to form magnetite and sodium aluminate phases under lower (5-10 %) hydrogen concentration. The transformation of hematite to magnetite and sodium aluminate formation is influenced by the temperature. From 400-500 °C, magnetite is the predominant Fe-bearing phase, while at >500 °C, the thermodynamic stability of the wüstite and pure iron phases rises. The thermodynamic phase stability of $NaAlO_2$ increases till 500 °C and the excess formation of sodium silicate and sodium iron oxides was observed. Based on the performed thermodynamic analysis, the temperature regime between 400 and 600 °C and with 20 wt % NaOH is favored for the enrichment of magnetite and sodium aluminate phases under hydrogen atmosphere in BR.

3.3 Phase transformation and Microstructural analysis

The XRD phase patterns of reduced BR under pure hydrogen by varying reduction time and NaOH addition at 500 °C are visible in Figure 2. To explore the effects of NaOH concentration, reduction roasting experiments were carried out with NaOH content (wt%) of 10 wt%, 15 wt%, 20 wt%, and 25 wt% at 500 °C for 30 min under pure hydrogen. The XRD patterns are shown in Figure 2a. The findings showed that hematite, cancrinite, and alumina oxides were significantly influenced by increasing NaOH concentration under hydrogen. With the gradual increase of NaOH content, the characteristic diffraction peaks of hematite and goethite disappeared, and it was indicated that these phases were transformed into magnetite under hydrogen reduction as expected according to Equation 4.

$$3Fe_2O_3 + H_2 = 2Fe_3O_4 + H_2O \qquad (4)$$

On the other hand, magnetite is gradually decreasing with increasing NaOH (> 20wt % NaOH) due to excess Na^+ ions that might react with iron oxide, promoting a new phase of sodium iron oxide ($NaFeO_2$) according to Equation 5.

$$Fe_2O_3 + Na_2O = 2NaFeO_2 \qquad (5)$$

During subsequent water leaching, water leachable $NaFeO_2$ immediately precipitates as hematite (Fe_2O_3) [12] and then negatively affects the recovery and grade of iron in the downstream process.

Therefore, only 20 wt % amount of NaOH should be added to BR for the formation of Fe_3O_4 and $NaAlO_2$ phases in a hydrogen atmosphere. The majority of the aluminum and silica reacted with NaOH, yielding water-leachable sodium aluminate (PDF 33-1200), sodium aluminum silicate (PDF 49-0003), sodium silicate (PDF 16-0818), and sodium-calcium silicate (PDF 23-0671) in addition to magnetite. The excess of sodium silicate and sodium iron oxides will probably dissolve in water and form contaminants, which further decrease the purity of the leach liquor. The diffraction peaks of perovskite remain stable even with the addition of 25 wt % NaOH. When the reaction is carried out with 10 - 15 wt % NaOH, the complex cancrinite phase is still present and indicates that the phase was not completely decomposed at this composition range, which negatively influences the Al and Na recovery. During reduction roasting, the Al^{3+} cations in the aluminum oxide phases, such as diaspore and gibbsite, diffuse towards the reaction zone where they combine with Na^+ to form water-soluble $NaAlO_2$ compounds according to Equations 6-7.

$$Al_2O_3 + 2\ NaOH \rightarrow 2\ NaAlO_2 + H_2O \quad (6)$$

$$Al_2O_3 + Na_2O \rightarrow 2\ NaAlO_2 \quad (7)$$

On the other hand, with increasing reduction time (as shown in Figure 2b), magnetite decreased, and iron and sodium iron oxide formed. The complete transformation of hematite to magnetite phase was found with a 30 min reduction time. In addition, the diffraction intensities of the characteristic sodium aluminate peaks were slightly enhanced by increasing the time factor. The typical diffraction peak strength of Fe_2O_3 decreases while that of Fe_3O_4 increases till 500 °C, suggesting that a temperature of at least 500 °C was necessary for full conversion of hematite to the desired magnetite. However, when the temperature is ≥600 °C, Fe_3O_4 is decreased and then transformed into wüstite, sodium iron oxide plus a minor metallic Fe-phase(A shown in figure 3). The diffraction intensities of characteristic $NaAlO_2$ peaks are increasing with increasing temperature. In addition, the diffraction peaks associated with anatase, quartz, diaspore, and perovskite did not change appreciably, indicating that at 400 °C, these phases did not undergo any reactions or transformations.

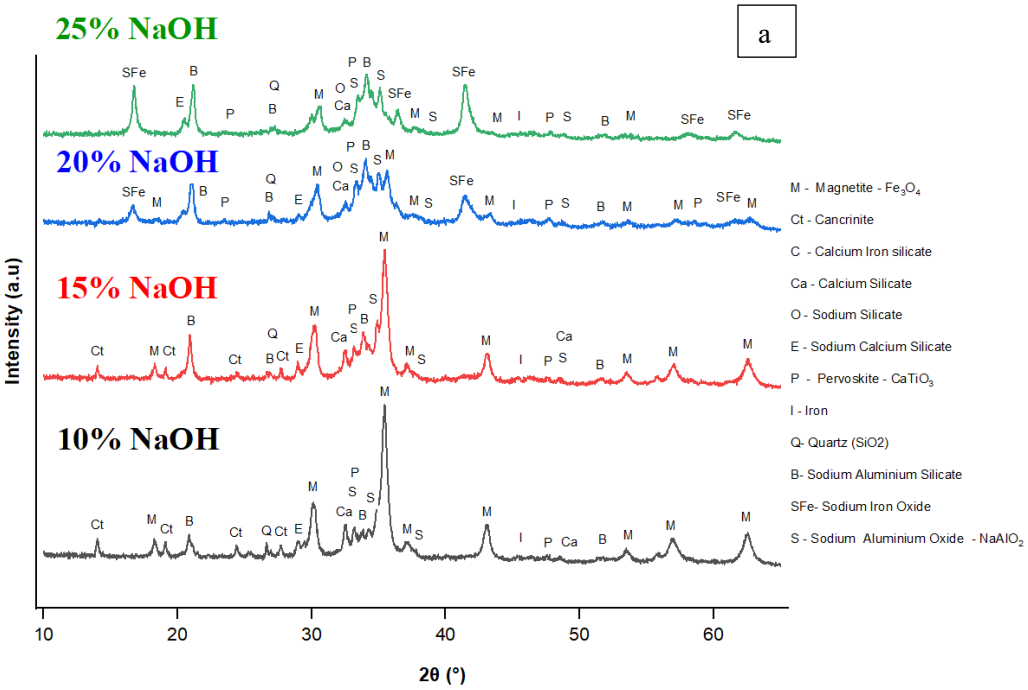

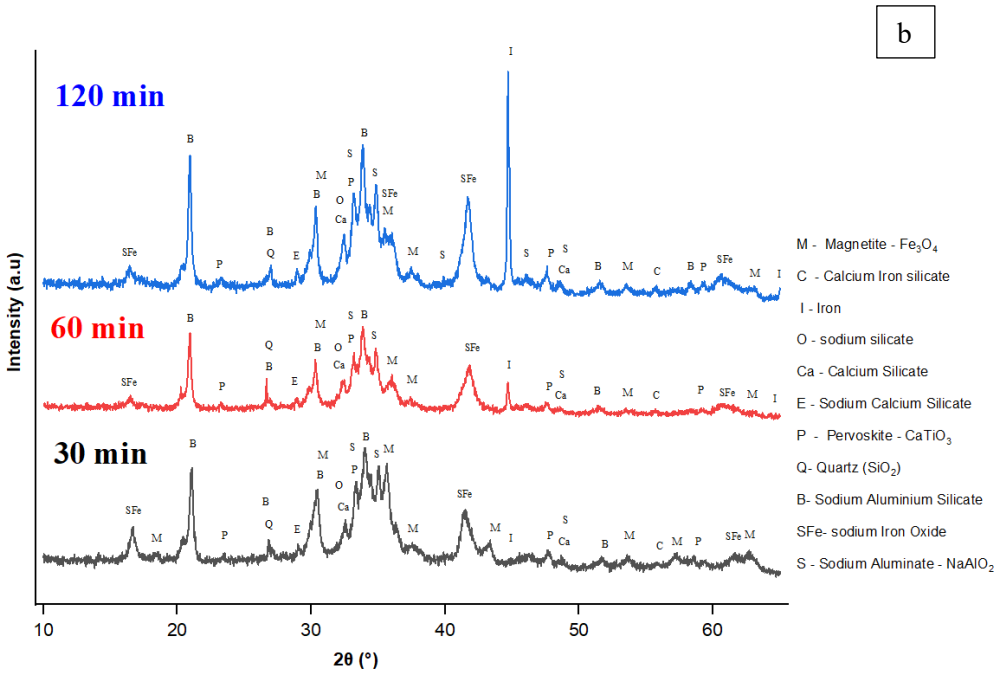

Figure 2. XRD patterns of the hydrogen reduced products obtained from changing a) NaOH addition b) reduction time at 500 °C.

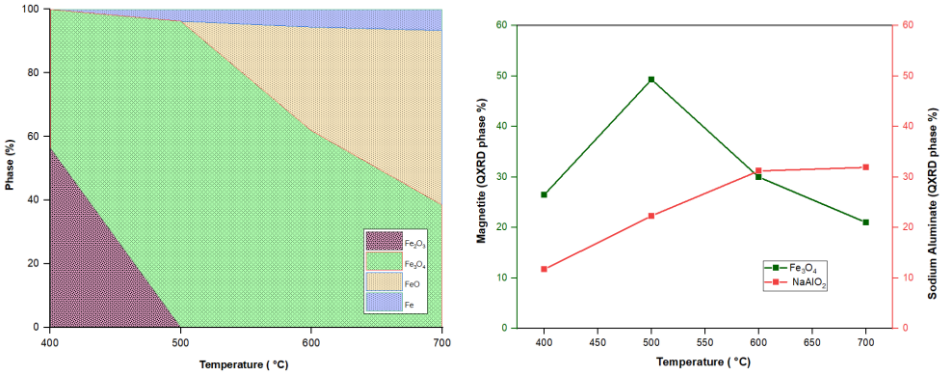

Figure 3. Effect of temperature a) QXRD phase quantification of Fe3O4 and NaAlO2 b) conversion degree (based on QXRD) of iron phases.

The XRD phase changes of magnetic and non-magnetic phases during downstream water leaching and the combined wet-magnetic separation process of reduced BR (at 500 °C, 20 wt % NaOH, 30 min reduction period) are displayed in Figure 4. Sodium aluminate had dissolved in water and formed an Al-Na-rich solution. In addition, strongly magnetic iron oxide particles like magnetite were concentrated in the iron concentrate with minor phases of impure perovskite ($CaTiO_3$) and ilmenite ($FeTiO_3$), while non-magnetic phases including quartz, perovskite, calcite, and andradite along with some magnetite were similarly concentrated in the non-magnetic stream. The magnetite (Fe_3O_4) phase diffraction peaks in nonmagnetic residues are substantially lower than those in the magnetic fraction. These results indicated that magnetic and non-magnetic phases were efficiently separated from the reduced BR by combined water leaching and magnetic separation.

Looking at the phases and microstructure of the 20 wt % NaOH reduced sample, fully reduced magnetite was present inside the BR matrix along with sodium aluminate phases. According to XRF analysis, the iron recovery and grade of magnetic rich fraction after water leaching -magnetic separation of reduced BR (at 500 °C, 20 wt % NaOH, 30 min reduction time) is 87.7 % and 44.5 (where the Fe_3O_4 content is 64 %) respectively, whereas the aluminum and sodium recovery at

these conditions is 75 % and 87 % based on ICP-OES analysis. However, with increasing the reduction temperature and time the recovery rates of aluminum and sodium were predicted to increase based on the XRD peak intensities. In contrast, the iron recovery and grades can be decreased due to the formation of undesirable non-magnetic wustite and water-soluble sodium iron oxide phases at 600 °C and 700 °C.

From the EPMA analysis, it was discovered that the perovskite and iron-rich phases like goethite and hematite in raw BR contain submicron-sized REEs (Sc, Th). The existence of REEs in iron oxide phases is also verified by other researchers [13, 14]. After hydrogen reduction roasting at 500 °C, 20 wt % NaOH, 30 min reduction time, followed by combined water leaching - magnetic separation process, the occurrence of Sc and Th in the magnetite as well as some Ferro-titanate ($FeTiO_3$) phases were observed, which leads to a lower recovery of REEs during downstream processing of the non-magnetic fraction. In the non-magnetic fraction, the REEs are mainly accumulated in perovskite ($CaTiO_3$) and in low amounts in other Fe-rich phases (Fe_3O_4, $FeTiO_3$), which is expected to be favorable for the subsequent recovery of REEs including Sc, and Ti. So, the higher incorporation of REEs and Sc into non-magnetic phases is expected to lead to higher recovery of REEs (including Sc).

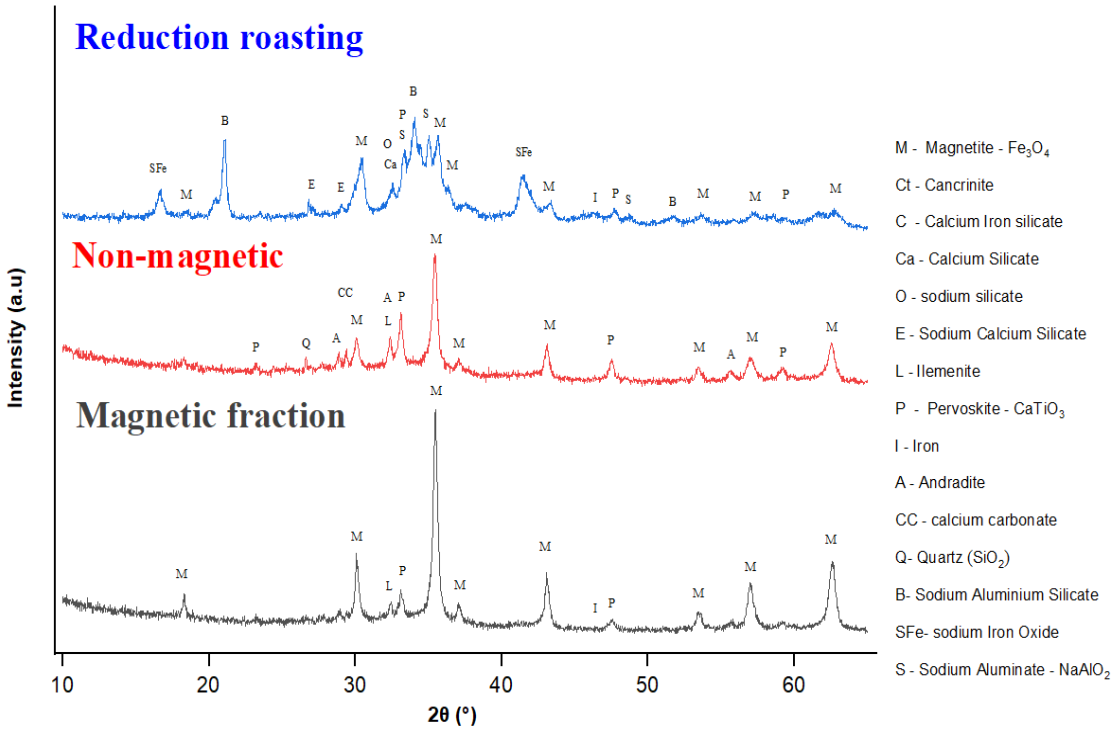

Figure 4. XRD patterns of reduced BR (at 500 °C, 20 wt% NaOH, 30 min reduction time), magnetic and non-magnetic residues after water leaching, and wet-magnetic separation.

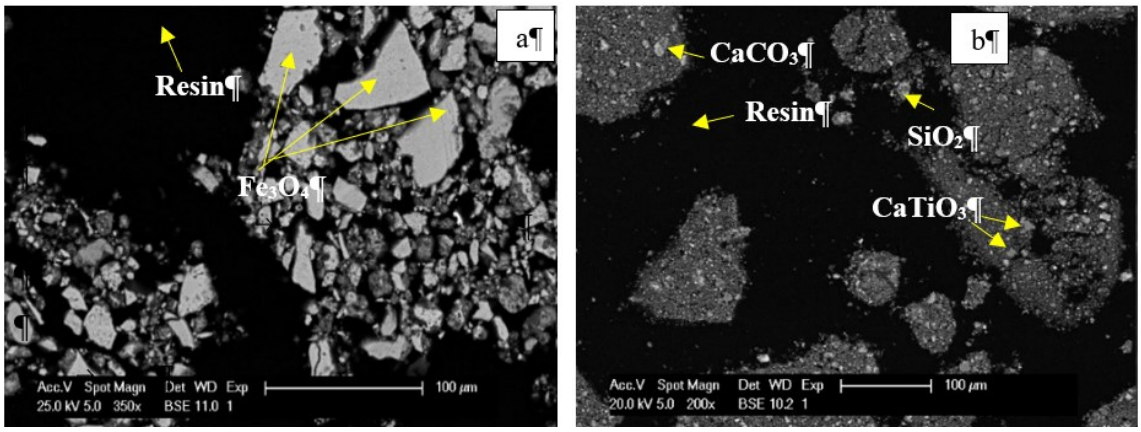

Figure 5. SEM microstructures of a) magnetic fraction b) non-magnetic residues after water leaching and wet-magnetic separation of reduced BR at 500 °C, 20 wt% NaOH, 30 min reduction time.

The SEM analysis on magnetic and non-magnetic fractions are depicted in Figure 5. The resulting iron fraction, which is rich in magnetite, is a value-added product for the iron industry or it can be utilized as a resource in the electrolytic refining of pure iron and other processes.

4. Conclusions

This paper investigated the reduction roasting behavior of various BR mineral phases under 100 vol % hydrogen by varying the NaOH dosage (10 - 25 wt % NaOH), reduction temperature (400 °C - 700 °C), and reduction time (30 - 120 min). Iron oxides (Fe_2O_3, FeOOH) and aluminum oxides (Al(OOH), $Al(OH)_3$), have been transformed into magnetite (Fe_3O_4), and sodium aluminates ($NaAlO_2$) after the reduction roasting process in the presence of 100 % vol. H_2 gas at a temperature and time of 500 °C and 30 min with 20 wt %. NaOH. The iron recovery and grade of magnetic rich fraction after water leaching -magnetic separation of reduced BR (at 500 °C, 20 wt % NaOH, 30 min reduction time) is 87.7 % and 44.5 (where the Fe_3O_4 content is 64 %) respectively, whereas the aluminum and sodium recovery at these conditions is 75 % and 87 %. The majority of the aluminum and silica reacted with NaOH, yielding water-leachable sodium aluminate ($NaAlO_2$), sodium silicate, sodium aluminum silicate, and sodium-calcium silicate, in addition to magnetite (Fe_3O_4) being the most common iron-containing phase during reduction roasting. Further, perovskite ($CaTiO_3$) remains a stable phase in all the reduction conditions. The efficient recovery of iron during the reduction process is hampered by the development of undesired sodium iron oxides ($NaFeO_2$) phases at ≥25wt % NaOH addition and by the formation of wustite (FeO) and sodium iron oxides ($NaFeO_2$) above ≥600 °C which was also observed in Factsage 8.1 thermodynamic investigation. Further research was done for the occurring transformations during the combined water leaching and wet-magnetic separation downstream process. Sodium aluminate ($NaAlO_2$) is dissolved in water, and three streams, namely magnetic fraction, non-magnetic fraction, and leach liquor, are yielded. With the aid of combined water leaching and wet magnetic separation, magnetite (Fe_3O_4) was concentrated in the magnetic concentrate, and non-magnetic phases like quartz (SiO_2), perovskite ($CaTiO_3$), ilmenite ($FeTiO_3$), calcite ($CaCO_3$), REEs (such as Sc, Th), andradite ($Ca_3Fe_2Si_3O_{12}$) with some magnetite, were enriched in the non-magnetic stream.

Acknowledgments

This project has received funding from the European Union's Horizon 2020 research and innovation programme under grant agreement No 958307. This publication represents exclusively

the authors' opinions, absolving the community of all responsibility. The Harare Project webpage is https://h2020harare.eu/.

5. References

1. Liu Xiao, Y. Han, F. He, P. Gao, S. Yuan., Characteristic, hazard, and iron recovery technology of red mud – A critical review, J. Hazard. Mater. 420 (2021) 126542.
2. Evans Ken, The history, challenges, and new developments in the management and use of bauxite residue, 2016, J Sustain Metall. 2(4):316–331.
3. Hannian Gu et al., Sequential extraction of valuable trace elements from Bayer process-derived waste red mud samples, 2018, J Sustain Metall 4:147–154.
4. Himanshu Tanvar, Mishra, B. Hydrometallurgical recycling of red mud to produce materials for industrial applications: Alkali separation, iron leaching and extraction. Metall Mater Trans 2021, B 52, 3543–3557.
5. Michael Archambo, S.K. Kawatra., Utilization of bauxite residue: recovering iron values using the iron nugget process, Miner. Process. Extr. Metall. Rev. 42 (4) 2021, 222–230.
6. Mingjun Rao, J. Zhuang, G. Li, J. Zeng, T. Jiang, Iron recovery from red mud by reduction roasting-magnetic separation, in B.A. Sadler (Ed.), Light Metals 2013, Springer International Publishing, Cham, 2016, pp. 125–130.
7. Chenna Rao Borra, B. Blanpain, Y. Pontikes, K. Binnemans., T. Van Gerven, Recovery of rare earths and major metals from bauxite residue (Red Mud) by alkali roasting, smelting, and leaching, J. Sustain, Metall. 3, 2017, 393–404.
8. Pilla Ganesh, R.K. Dishwar, S. Agrawal, A.K. Mandal, N. Sahu., O. Sinha, Feasibility of nickel extraction from Indian chromite overburden by solid-state reduction and smelting route, Journal of mining and metallurgy section b: metallurgy, 2020, 56 (2020) 229–235.
9. Michail Samouhos, M. Taxiarchou, G. Pilatos, P.E. Tsakiridis., E. Devlin, M. Pissas, Controlled reduction of red mud by H_2 followed by magnetic separation, Miner. Eng. 105, 2017, 36–43.
10. Chiara Cardenia, E. Balomenos, and D. Panias., Iron recovery from bauxite residue through reductive roasting and wet magnetic separation, J. Sustain. Met., 2018, vol. 5, pp. 9–19.
11. Stergi Kapelari, Platon, N. G., Tom Van, D.D., Yiannis, P., Bart, B, H_2 – based processes for Fe and Al recovery from bauxite residue (red mud): comparing the options. Mater. Proc.2021,5, 45.
12. Ganesh Pilla, S.V. Kapelari, T. Hertel et al., Hydrogen reduction of bauxite residue and selective metal recovery, Materials Today: Proceedings 57, 2022, 705–710.
13. Hossein Habibi, Pirouzan, D., Shakibania, S. et al., Physical and chemical separation of Ti, rare earth elements, Fe, and Al from red mud by carbothermal reduction, magnetic separation, and leaching. Environ Sci Pollut Res , 2022.
14. Johannes Vind, Malfliet, A., Blanpain, B., Tsakiridis, P.E., Tkaczyk, A.H., Vassiliadou, V., Panias, D., Rare earth element phases in bauxite residue, *Minerals* 2018, *8*, 77.
15. Xinbo Yang, Honaker, R.Q., Leaching kinetics of rare earth elements from fire clay seam coal. *Minerals* 2020, *10*, 491.